

Light and Electron Microscopy Study of Opportunistic Free-Living Nematodes Scavenging and Thriving within Buried Dinosaur Bones

Mark H. Armitage

DSTRI, Inc., 325 East Washington Street #170, Sequim, WA 98382

profmark@dstri.org

Abstract: Nematode worms are the most abundant multicellular organism on Earth. They thrive in every habitat known, and they are voracious feeders within the top 70 cm of soils. Their sturdy cuticle protects them from environmental factors and predators. Nematodes play a significant role in the decomposition of vertebrate remains in soil and serve as indicators of nutrients that enter soils during decomposition. Certain parasitic nematodes have been identified in fossil remains, but reports of fossil worms are rare. We demonstrate the abundant presence of opportunistic nematodes feeding within dinosaur bones from the Hell Creek formation, MT. The presence of visible worm ultrastructure indicates that they were alive when preserved within the dinosaur bones. Our findings are identical to worms characterized as “blood parasites” in a dinosaur bone from Brazil, demonstrating that there is sufficient soft tissue within dinosaur bone canals to sustain large populations of nematodes post-mortem.

Keywords: nematodes, Hell Creek Montana, dinosaur, vasculature, bone canals

Introduction

Nematodes (Figure 1), often called roundworms, are the most abundant multicellular life form on Earth. The “father of nematology,” Nathan Cobb, famously wrote, “In short, if all the matter of the universe except the nematodes were swept away, our world would still be dimly recognizable, and if, as disembodied spirits, we could then investigate it, we should find its mountains, hills, vales, rivers, lakes, and oceans represented by a film of nematodes.” [1]

It was estimated in 2017 that a million undescribed species exist in this ubiquitous group of soil organisms. That number may be far too low. A recent survey [2] of over 6700 soil samples estimated that there are 57 billion nematodes for every living human being on Earth. They are found in every habitat, can feed on many sources, and their seeming impermeability to hazards from foes and nature is astonishing. Nematodes can be frozen for weeks, and, once revived, can resume their prodigious reproduction schedule unimpeded [29].

The earliest reports regarding nematode infections of humans date to writings from Chinese medicine in 2700 BC and from the Egyptian Papyrus Ebers (1550 BC) [8]. The current literature describing these organisms is voluminous, therefore the reader is encouraged to review cited works for background on their biology [3–19]. Nematodes are generally categorized by the types of feeding they conduct and the substrates upon which they feed. Many are free-living and opportunistic omnivores [4,7,9,10] that feed upon bacteria, fungi, algae, plants, animals, and even each other [6–8]. Some are strictly human parasites [13–19], and others infect and parasitize only insects. In many cases the same insects destroy plant crops globally [6–7,12,20–26].

The abundance (and permanence) of nematodes might be related to the ultrastructure of their cuticle. The nematode cuticle is a complete covering, variable in both thickness and numbers of layers. It is somewhat like a puncture-resistant bag that encapsulates and protects the nematode from predators and the environment [20–24]. Two to three layers of unique tissues make up the cuticle complex, and worms with 4- to 7-layer cuticles are common [20–21]. Workers have noted that the cuticle inhibits proper fixation and infiltration during lab processing for microscopy [20]. The cuticle is also known to thicken post-mortem in some nematodes [27]. The cuticles of nematodes that died in distilled water swelled significantly, while some were desiccation-tolerant when water loss was gradual [20]. These tough nematode cuticles might be the reason why many plant parasitic nematodes are so successful [25–26] and our management of them is not.

Nematodes play a large role in the decomposition of vertebrate cadavers that enter or lie upon soils [10,28–31]. Cadaver presence in soil is characterized by increased biomass due to microbial, fungal, and nematode activity, particularly if the cadaver is on the surface [10]. This increase persists over time and is supplemented by the introduction of fecal matter, dead insects (all life-cycle stages), feathers, hair, fur, etc., by decomposers attracted to the site [10]. Burial below the surface restricts access to most scavengers and insects [28,30]. This is known to retard cadaver decomposition, however, 70% of nematodes are known to live under the soil surface, in the top 20–30 cm of soil [10,28], and they play a large role in decomposition. Nematodes become undetectable below 85 cm soil depth. Bacterial growth, as a result of nutrient pulses from a cadaver, is sufficient to boost free-living nematode populations. Burial at depths below 40 cm slows decomposition due to restrictions placed on above-ground insect scavengers. In this way, preservation of cadavers can persist for thousands of years [10], and soft tissues can remain for long periods [30]. One forensics report analyzed nematode abundance under human remains in a Swiss forest and noted that the highest density of nematode populations occurred under the cadaver head, while most nematode *diversity* was clustered below the upper body [29]. Those workers observed no soft tissue on the outside of the skeleton and deduced that it had been in the forest for less than a year, however, no mention of soft tissue within the bones was made. Interestingly, carbon compounds such as sugars, lipids, and proteins are consumed rapidly by microbes, such that cadaver fluids do not generally persist below the topsoil [31].

Recognizable parasitic nematode forms are represented in fossil remains, but reports are sparse [32–42]. There exists enough material, however, to establish their presence within the Mesozoic era, but little in the Paleozoic [34,35]. “Nematode-like” structures

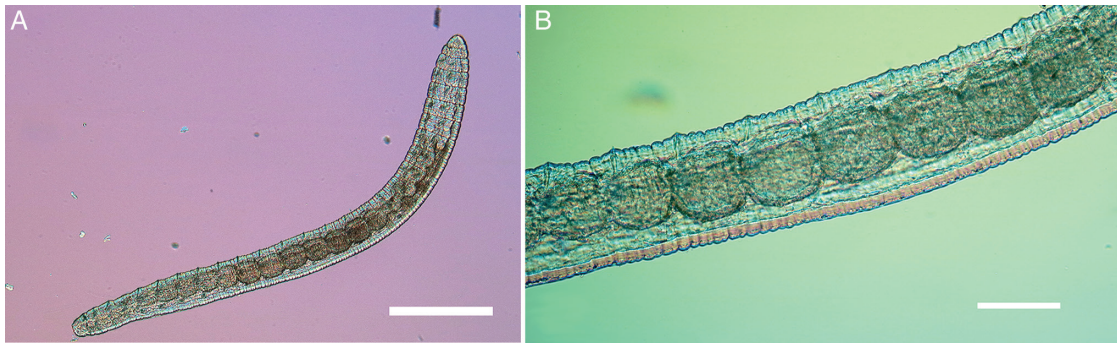


Figure 1: Light micrographs of nematode collected and processed by the Baermann funnel method. Note cuboidal ovaries in B. A, scale bar = 300 μm . B, scale bar = 75 μm .

have been observed in Precambrian rocks, but clear examples of nematodes are not noted. Reports from the late Mississippian era [37,38] are clearer. Either way, corroboration is scarce.

Recently, a claim was made for the “first record of a parasite inside fossilized bone,” even though the bone was infiltrated by calcite and permineralized [42]. A Brazilian titanosaur fibula fragment had evidence of bacteria-caused osteomyelitis on its outer surfaces as well as multiple “fusiform shapes” (described as trypanosomids) within bone canals. If corroborated, these would be by far the largest trypanosomes discovered [43]. We interpret the “trypanosomes” as the tough cuticular and other remains of opportunistic, free-living nematodes [20–24, 43–45] that migrated from the soil into dinosaur bones after burial to scavenge resources found within. If nematodes are present within dinosaur bones in Brazil, the present work might be a corroboration at the North American deposits at Hell Creek. The purpose of this paper was to examine thin sections of bones of *Triceratops*, *Nanotyrannus*, and *Edmontosaurus* removed from soil at Hell Creek, MT for the presence of nematodes.

Materials and Methods

We collected fresh scapula (DSTRI#5622-ES), jaw (DSTRI#5622-EJ), and rib (DSTRI#5622-ER) from *Edmontosaurus annectans* at Hell Creek formation, Glendive, Montana, during the summer of 2022. The *Edmontosaurus* skeleton was complete and measured approximately 27 feet in length, possibly because it came to lie as if folded over on itself. Bones were immersed in formalin at the site and transported to the lab for further processing. Specimens were washed, air-dried, and 40 μm ground sections (uncoated) were prepared. Non-cover-slipped sections were viewed under brightfield, polarized light, and SEM in backscattered electron mode and examined for the presence of fusiform nematode cuticles in vascular canals. We examined these fusiform shapes for several identifying characteristics, including location, size, width, one end more tapered than the other, and dark internal spots [42]. Additionally, we sampled previously collected specimens of *Triceratops horridus* and *Nanotyrannus lancensis* [45,46] from Hell Creek, including *Nanotyrannus* rib (DSTRI#831-H) and vertebra (DSTRI#91-C) and *Triceratops* horn (DSTRI#HCTH-03), rib (DSTRI#HCTR-11), vertebra (DSTRI#HCTV-22), and frill (DSTRI#HCTF-39). We similarly sampled a *Triceratops* condyle previously examined for nerves [47] (DSTRI#HCTH-44).

Results

All thin sections examined microscopically contained nematodes (Figures 2–12). Nematodes ($n = 217$) were always found in vascular canals, displayed a grey/green color in brightfield, were fusiform in shape, had one end more tapered than the other, had internal dark spots, and measured 100–600 microns in length and 10–80 microns in width. The shortest worms observed were 8 microns in length and were also the widest, suggesting a behavioral contraction (Figures 5C and 3D, left side) prior to, or as a result of, preservation within the canal. Nematodes mostly infested canals containing a brown crystallized material adhering to the bone canal walls (Figure 7A). This brown material glowed brightly in UV autofluorescence (Figures 3D and 5D), indicating that they are iron-rich clots. These canals must still have proteins within them that attract fungi (Figure 6A) and certainly bacteria for decomposition. Moreover, many canals had multiple worms of varying sizes, suggesting an environment conducive for reproduction. This is evidenced by the presence of smaller worms, which we interpret to be juveniles (Figures 3A, 4D, 6C). Internal dark spots were present in most worms, often as one large spot and sometimes as two or more small spots. Many worms also displayed complex internal structure, indicating they were alive when fixed (Figures 6C, 7B, 7C, 11D, 12A).

Discussion and Conclusions

We find that bones collected at Hell Creek, MT are rarely or only lightly permineralized, which might contribute to soft tissue abundance and would allow free access to opportunistic scavengers such as fungi, bacteria, and nematodes. Bones in this condition might also support an environment conducive for reproduction and population increase if ample food sources are available. If in-bone resources are plentiful we would expect nematode offspring to be present and at differing stages of growth, as evidenced by the varying sizes of fusiform shapes in blood canals described here and by Aureliano et al. in the titanosaur fibula [42]. That study proposed 6 characteristics of the fusiform microorganisms found in the Brazilian bone canals. Five of the six characteristics matched the forms we found in Hell Creek specimens. These include grey/green color of the shapes in brightfield, fusiform body shape, always being found only in vascular canals, one end being more tapered than the other, internal dark spots, and measurements of 100–600 microns in length and 10–80 microns in width. Worms in the titanosaur displayed irregular anisotropy, unlike the Hell Creek worms which

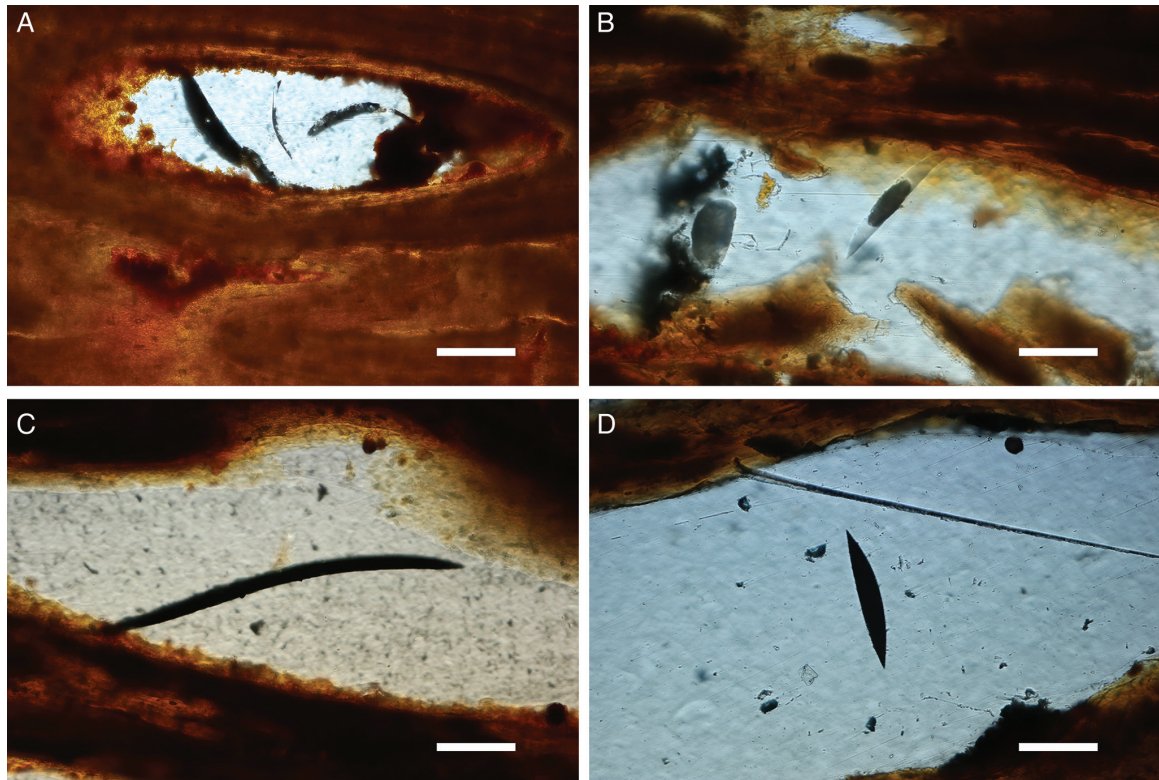


Figure 2: Thin sections showing four examples of nematode infestation from bone canals of *Edmontosaurus* scapula. Scale bars = 24 μ m.

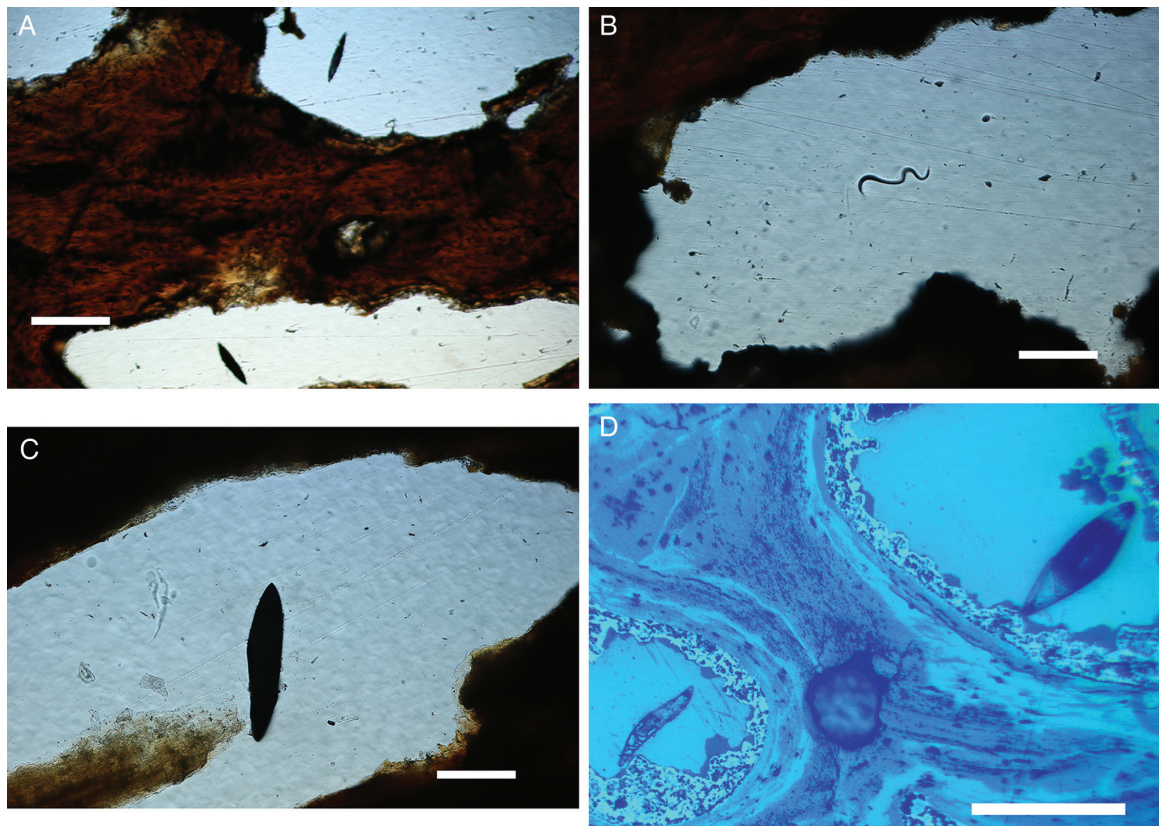


Figure 3: Thin sections of nematode infestation from bone canals of *Edmontosaurus* jaw. A, B, and C, light micrographs. D, UV fluorescence showing bright clots adhering to the canal walls. A and B, scale bar = 24 μ m. C, scale bar = 10 μ m. D, scale bar = 20 μ m.

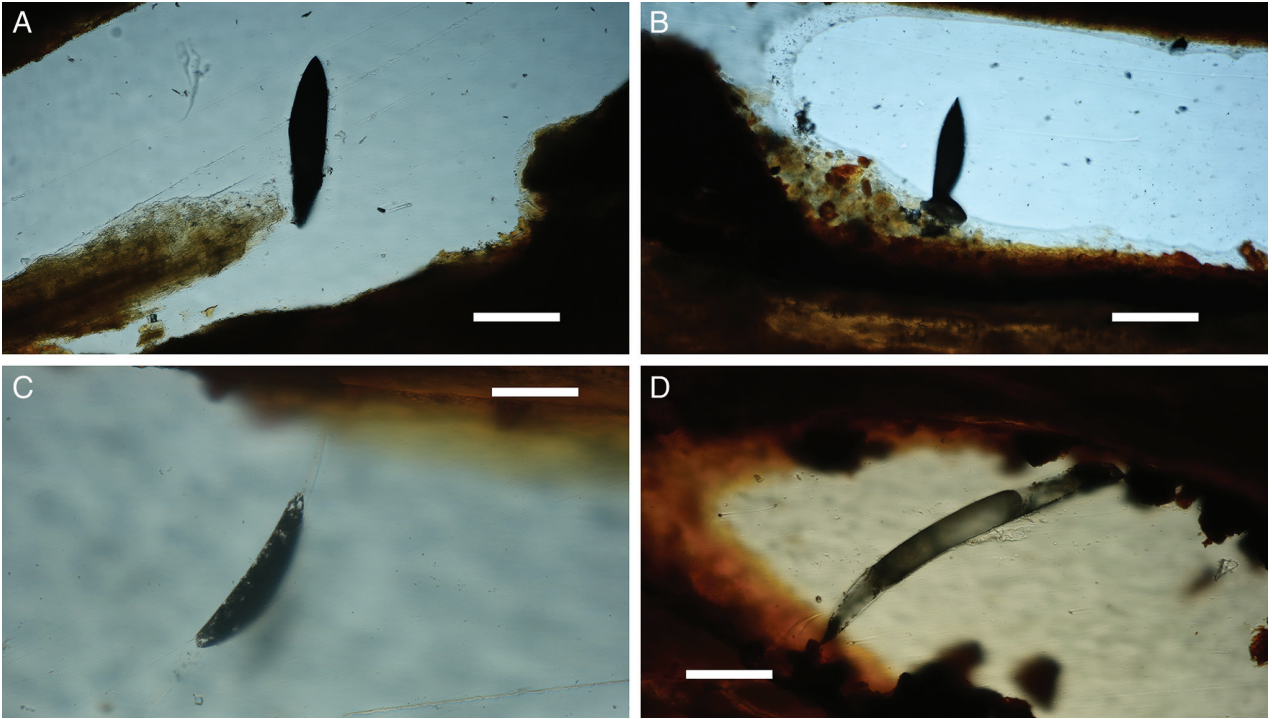


Figure 4: Thin sections showing four examples of nematodes in the *Edmontosaurus* rib bone canal. Scale bars = 12 μm .

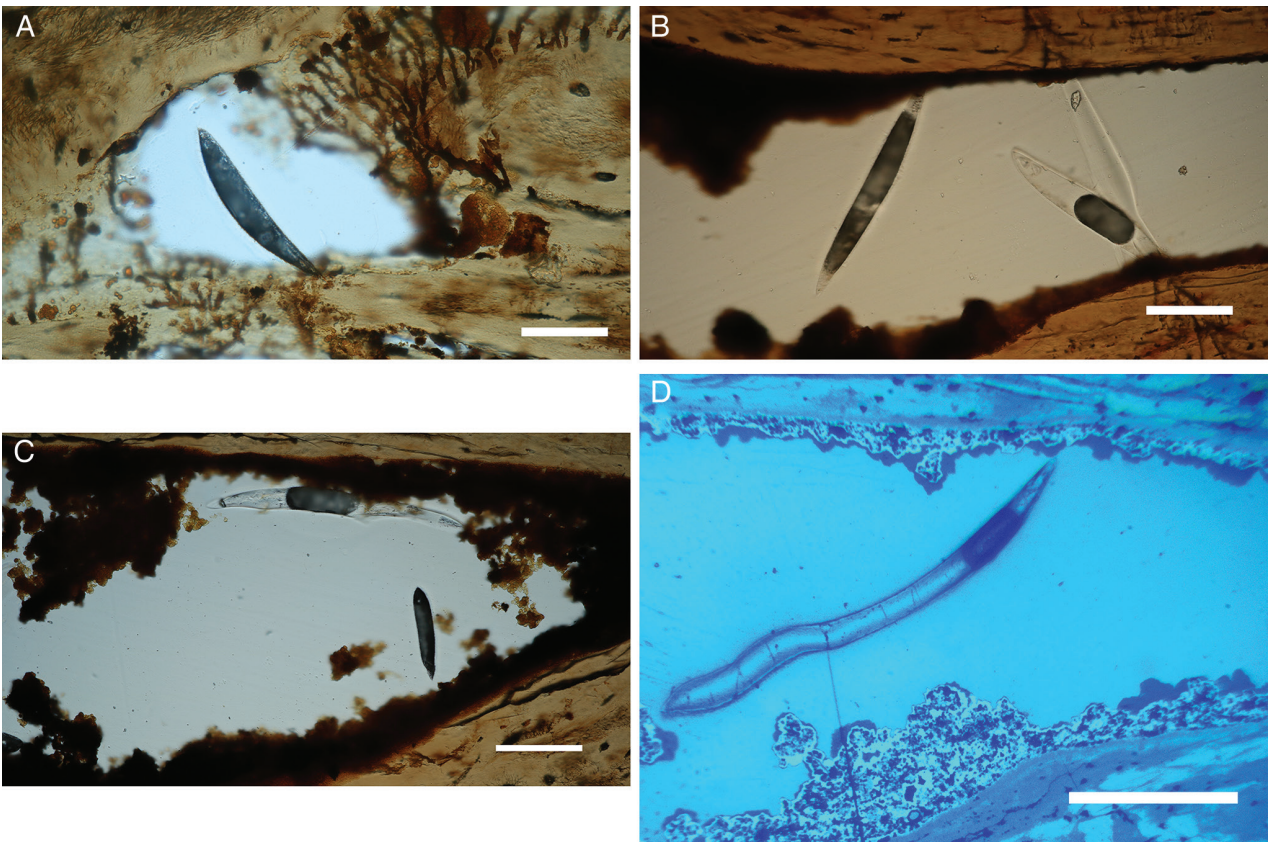


Figure 5: Thin sections showing four examples of nematodes in the rib bone canals of *Nanotyurannus*. A, note the dark brown fungal hyphae penetrating the bone to the right of the canal. D, UV fluorescence image shows the autofluorescent clot adhering to the canal wall. A and B, scale bar = 10 μm . C, scale bar = 7 μm . D, scale bar = 25 μm .

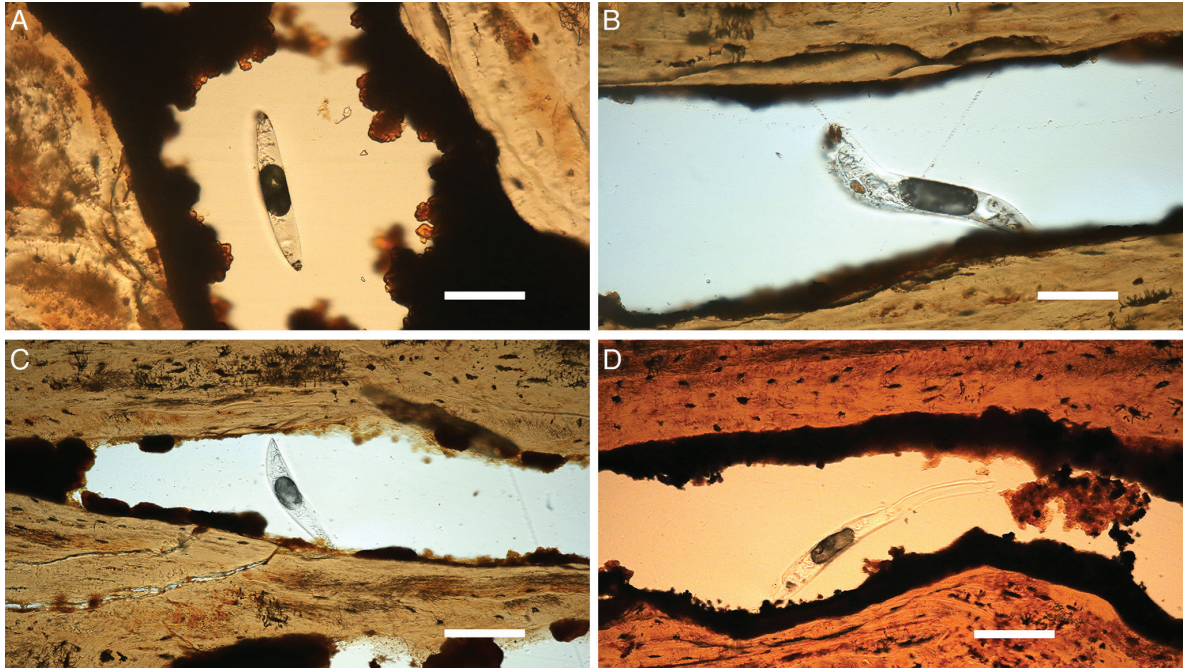


Figure 6: Thin sections showing 4 examples of nematodes from the vertebra bone canals of *Nanotyrranus*. A and C, scale bars = 12 μm . B and D, scale bars = 15 μm .

are isotropic [42]. This might be an artifact of processing in the Brazilian work due to the use of cyanoacrylate glue (PaleoBOND) to infiltrate the bone or more probably because calcite was present in canals. We fix at the site and use no cyanoacrylate, and calcite permineralization is rare at Hell Creek. Therefore, canals are generally clear of debris or detritus (Figures 4–12).

Characteristics of nematodes shown here closely match observations made on nematodes within the titanosaurus fibula, except for the presence of calcite. We do note one characteristic not mentioned by Aureliano et al. [42]. In their figures 5A–H, we observed that all fusiform shapes are associated with brown material in the vascular canals. We interpret the brown material

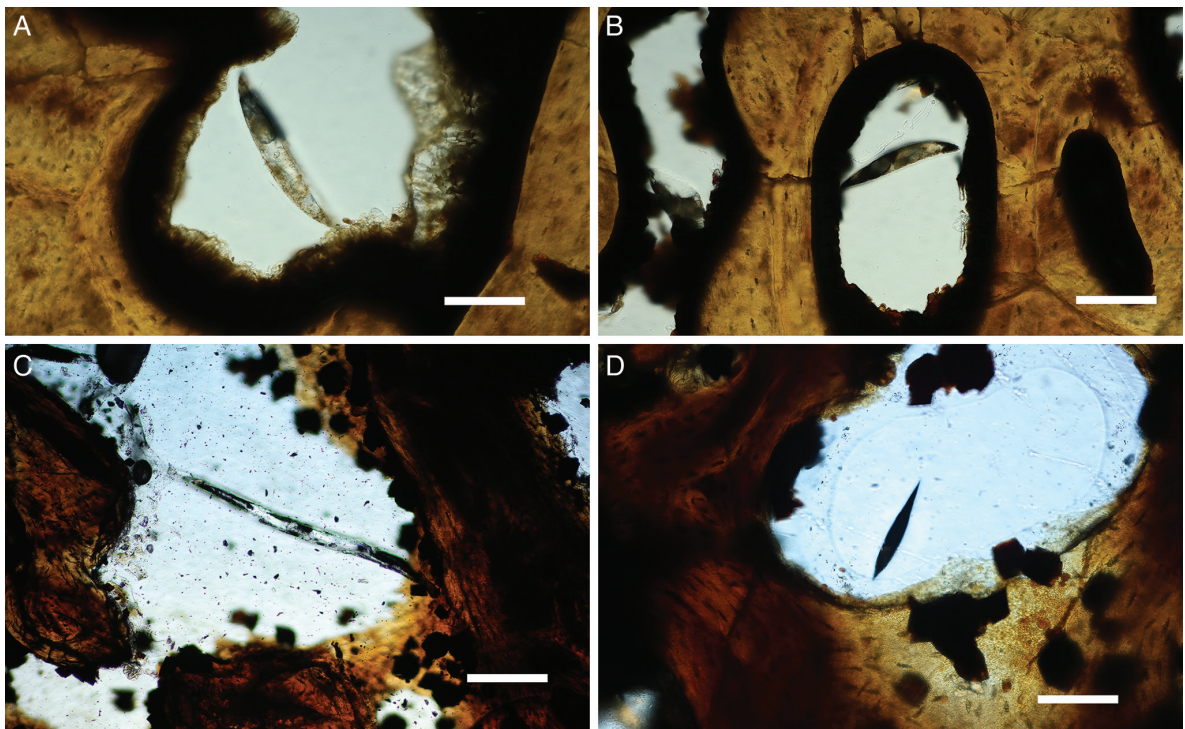


Figure 7: Thin sections showing four examples of nematode infestation from the of condyle bone canals of *Triceratops*. Scale bars = 12 μm .

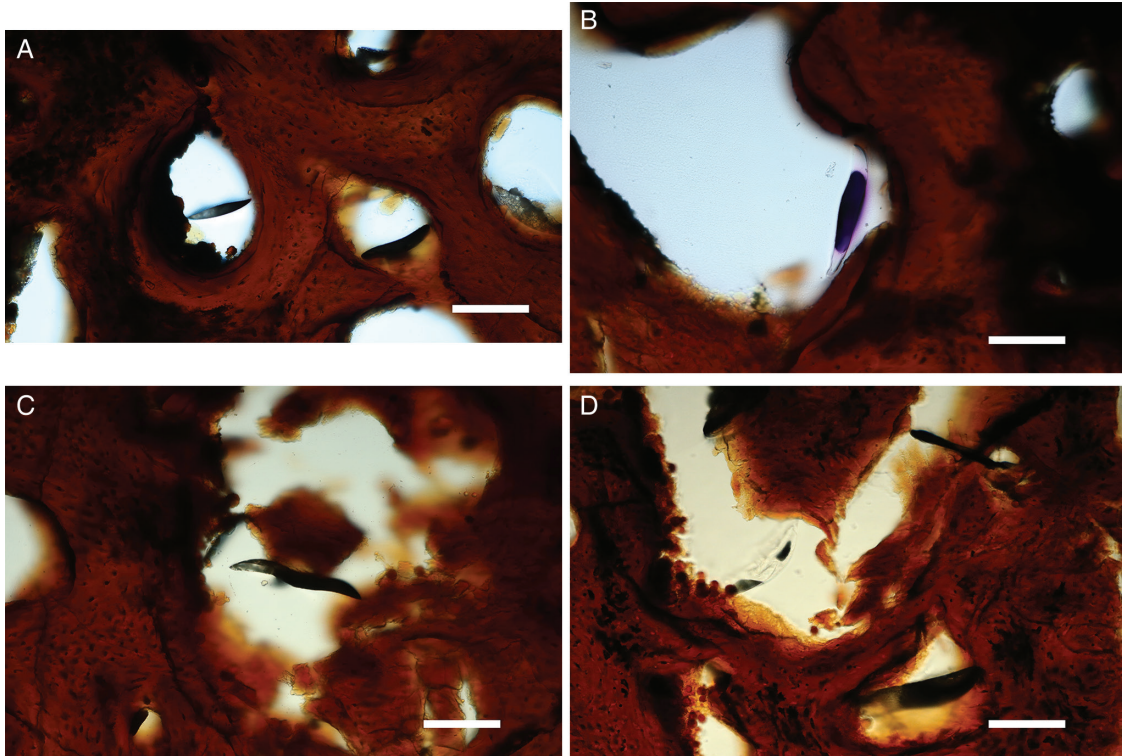


Figure 8: Thin sections showing four examples of nematode infestation from the frill bone canals of *Triceratops*. Scale bars = 12 μm .

to be the remains of blood clots described by us previously [45,46]. This suggests that both the titanosaur bone from Brazil and the *Triceratops*, *Nanotyrannus*, and *Edmontosaurus* specimens studied here suffered identical infestation by opportunistic nematodes living in the soil where the bones came to be buried. We suspect

that the dark spots are the remains of nematode organelles that experienced putrefaction within the cuticle of the nematodes. As discussed, the highly resistant cuticle even impedes infiltration of fixative [20], therefore worms that came in contact with fixative may have sealed themselves off in an attempt to impede the action

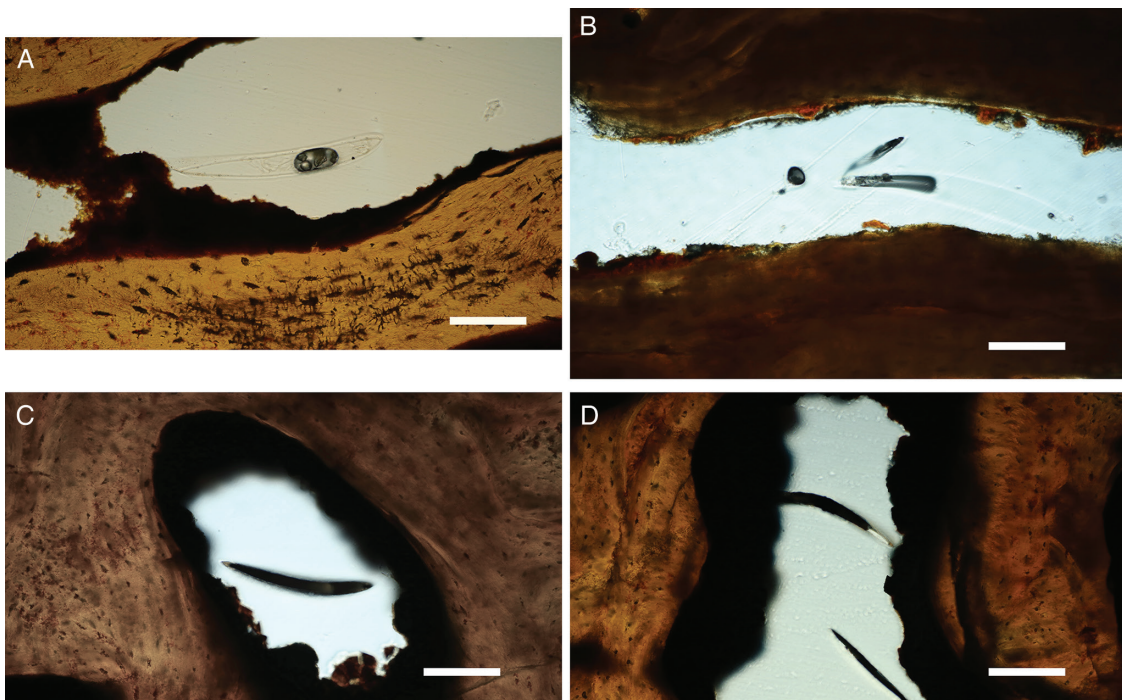


Figure 9: Thin sections showing four examples of nematode infestation from the horn bone canals of *Triceratops*. A, scale bar = 12 μm . B, C, D, scale bar = 10 μm .

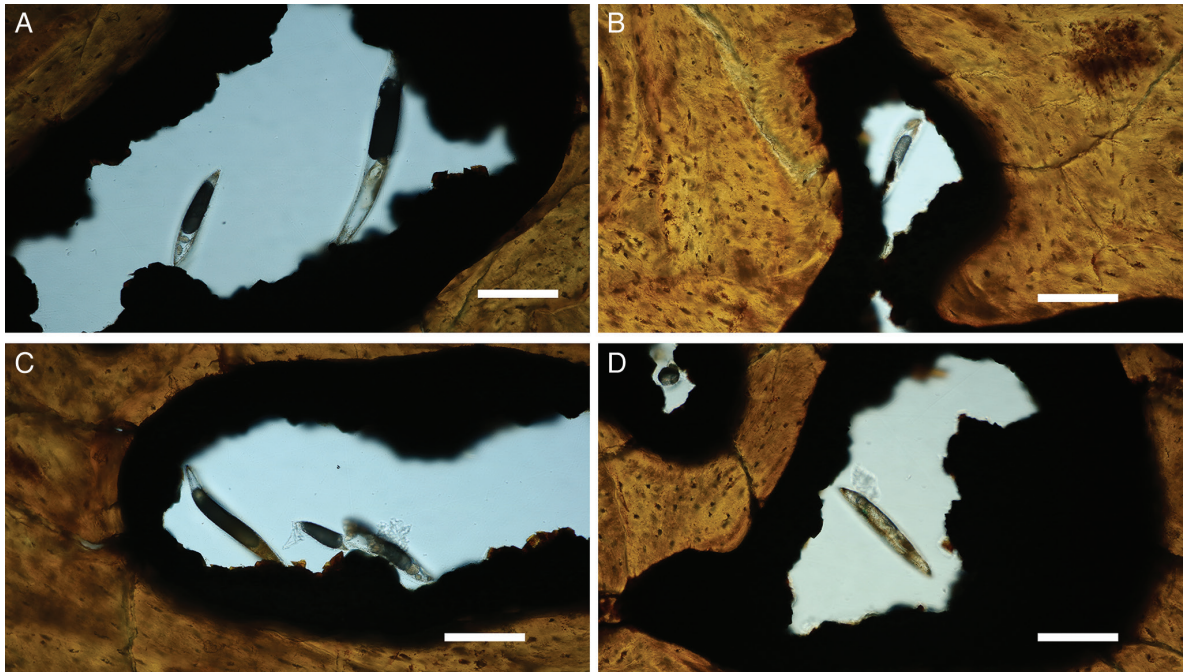


Figure 10: Thin sections showing four examples of nematode infestation in the rib bone canals of *Triceratops*. Scale bars = 12 μ m.

of the fixative. We also examined thin sections containing canal nematodes using back-scattered electron imaging (Figure 12B). The top of the nematode cuticle was removed during sectioning revealing two cuboidal structures within the body of the worm. These cuboidal shapes resemble nematode ovaries present in living worms (Figure 1B). More studies must be done to corroborate

the presence of what we interpret to be living opportunistic nematodes feeding within the Hell Creek dinosaur bones shown here.

Acknowledgements

We want to thank Dr. Robert Price and other anonymous reviewers for making this a better manuscript. We also acknowledge

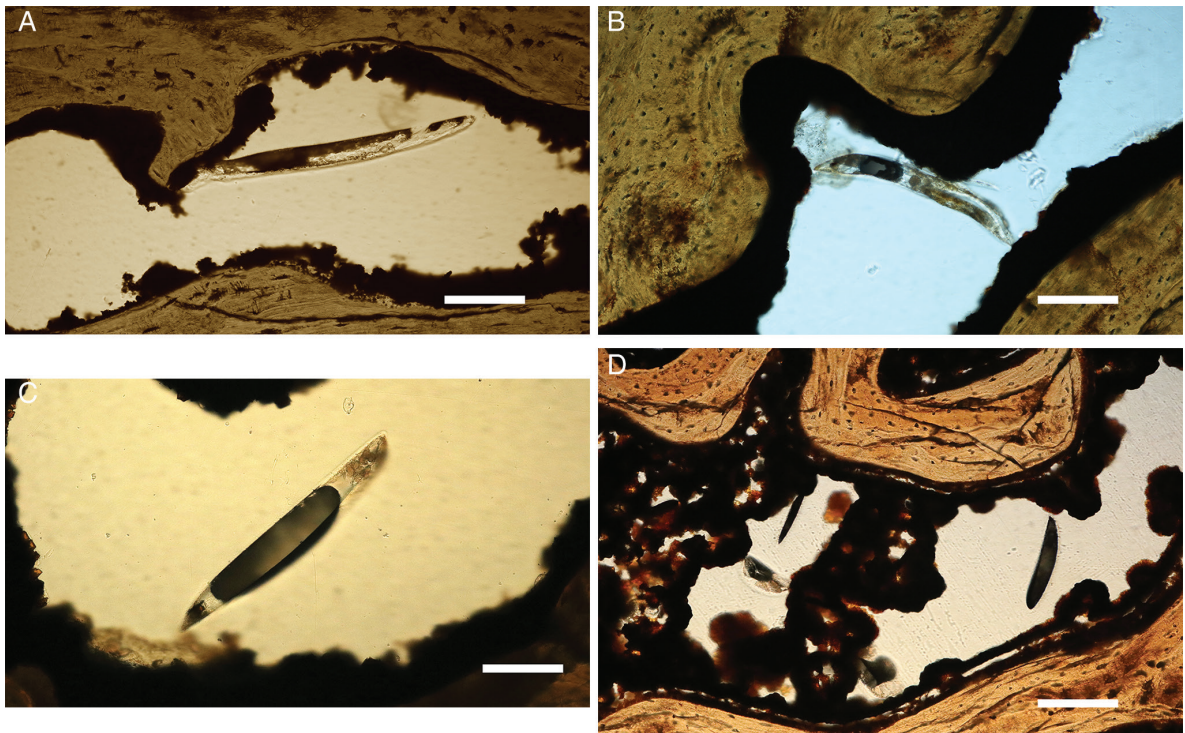


Figure 11: Thin sections showing nematode infestation in the vertebra bone canals of *Triceratops*. A, B, D, scale bar = 12 μ m. C, scale bar = 10 μ m.

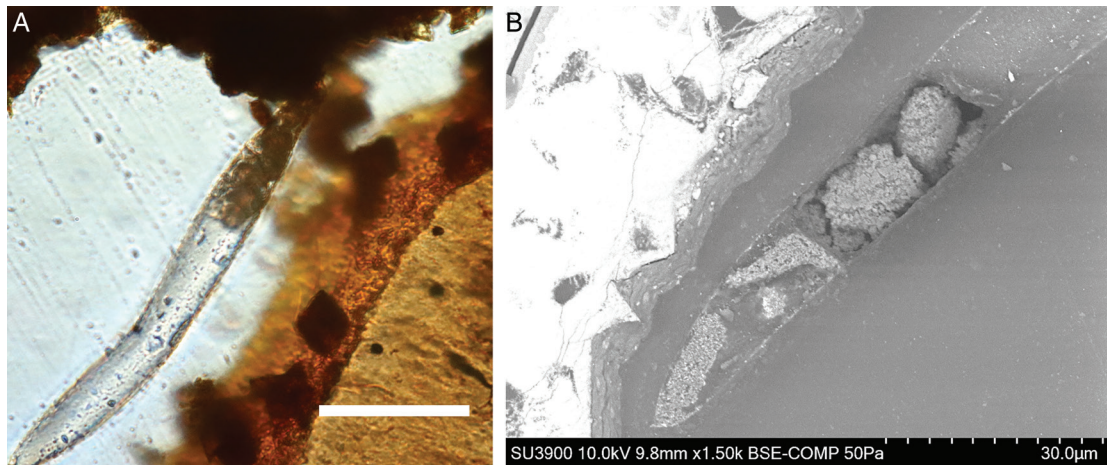


Figure 12: A, thin section showing nematode infestation from the vertebra bone canal of *Triceratops*. B, SEM backscattered electron image showing nematode infestation in a vertebra bone canal from *Triceratops*. Note cuboidal structures (possible ovaries) within the body of the nematode. Scale bars = 30 µm.

the valuable assistance of the Hitachi team that performed the SEM-BSE work on these specimens, including Maurilio Martinez, Senior Manager Analysis Systems, Yuki Tani, Applications Engineer II, and Summer Hamilton, Hitachi STEM coordinator.

References

- [1] NA Cobb, *Nematodes and their relationships* (1914), U.S. Government Printing Office.
- [2] J van den Hoogen et al., *Nature* 572 (2019) <https://doi.org/10.1038/s41586-019-1418-6>.
- [3] NA Cobb, *Transact Amer Microsc Soc* 33 (1914) <https://www.jstor.org/stable/3221617>.
- [4] IN Filipjev, *Smithsonian Misc Collect* 89 (1934) https://repository.si.edu/bitstream/handle/10088/23985/SMC_89_Filipjev_1934_6_1-57.pdf.
- [5] J Hodgkin, *Genetics* 121 (1989) <https://doi.org/10.1093/genetics/121.1.1>.
- [6] R Alkemade et al., *Mar Ecol Prog Ser* 105 (1994) <https://www.int-res.com/articles/meps/105/m105p277.pdf>.
- [7] L Armendariz and P Arpin, *Biol Fertil Soils* 23 (1996) <https://doi.org/10.1007/BF00335914>.
- [8] N Greco and A Marinari, *Redia* 94 (2012) <https://api.core.ac.uk/oai/oai:journals.crea.ugov.it:article/654>.
- [9] S Cesarz et al., *Soil Organisms* 91 (2019) <https://doi.org/10.25674/so91201>.
- [10] LS Taylor, et al., *PLoS ONE* 15 (2020) <https://doi.org/10.1371/journal.pone.0241777>.
- [11] SC Tintori et al., *J Vis Exp* 179 (2022) <https://doi.org/10.3791/63287>.
- [12] J Desaeger, et al., *J Nematol* 55 (2023) <https://doi.org/10.2478/jofnem-2023-0018>.
- [13] K Mohammed et al., *Intl J Path Res* 12 (2023) <https://doi.org/10.9734/IJPR/2023/v12i2220>.
- [14] A Ridall and J Ingels, *Environ Monit Assess* 195 (2023) <https://doi.org/10.1007/s10661-023-11555-5>.
- [15] MS Panayotova-Pencheva, *Acta Morphol Anthropol* 30 (2023) <http://iempam.bas.bg/journals/acta/acta30a/116-121.pdf>.
- [16] D Buonfrate et al., *Eurosurveillance* 23 (2018) <https://doi.org/10.2807/1560-7917.ES.2018.23.16.17-00527>.
- [17] HU Pangaribuan et al., *Maj Kedo Band* 53 (2021) <https://doi.org/10.15395/mkb.v52n4.2545>.
- [18] S Caldrier et al., *Microorganisms* 10 (2022) <https://doi.org/10.3390/microorganisms10051027>.
- [19] EE Imalele et al., *Parasitol Res* 122 (2023) <https://doi.org/10.1007/s00436-023-07809-3>.
- [20] IKA Ibrahim, *LSU Historical Dissertations and Theses* 1251 (1967) https://doi.org/10.31390/gradschool_disstheses.1251.
- [21] PW Johnson et al., *J Nematol* 2 (1970) <https://pubmed.ncbi.nlm.nih.gov/19322273>.
- [22] AF Bird, *The Nematode Cuticle and Its Surface, in Nematodes as Biological Models: Aging and Other Model Systems, vol. 2*, BM Zuckerman, ed. (1980) Academic Press New York, NY, ISBN: 0-12-782402-2.
- [23] E Karanastasi et al., *Helminthologia* 45 (2008) <https://doi.org/10.2478/s11687-008-0019-y>.
- [24] K Ichiishi et al., *Nematology* 24 (2022) <https://doi.org/10.1163/15685411-bja10196>.
- [25] Q Li et al., *Front Plant Sci* 14 (2023) <https://doi.org/10.3389/fpls.2023.1173157>.
- [26] C Khanal and J Land, *Sci Rep* 13 (2023) <http://doi.org/10.1038/s41598-023-41466-x>.
- [27] AM Koppenhöfer et al., *Appl Soil Ecol* 6 (1997) [https://doi.org/10.1016/S0929-1393\(97\)00018-8](https://doi.org/10.1016/S0929-1393(97)00018-8).
- [28] DO Carter et al., *Naturwissenschaften* 94 (2007) <https://doi.org/10.1007/s00114-006-0159-1>.
- [29] I Szelezcz et al., *Sci Rep* 8 (2018) <https://doi.org/10.1038/s41598-017-18179-z>.
- [30] SW Keenan et al., *PLoS ONE* 13 (2018) <https://doi.org/10.1371/journal.pone.0208845>.
- [31] S Fiedler et al., *Front Soil Sci* 3 (2023) <https://doi.org/10.3389/fsoil.2023.1107432>.
- [32] GO Poinar, *J Parasitol* 70 (1984) <http://www.jstor.org/stable/3281883>.
- [33] GO Poinar et al., *Fund Appl Nematol* 17 (1994) https://horizon.documentation.ird.fr/exl-doc/pleins_textes/fan/40786.pdf.
- [34] CC Labandeira, *Paleontol Soc Papers* 8 (2002) <https://doi.org/10.1017/S1089332600001108>.

- [35] GO Poinar, *J Nematol* 35 (2003) <https://www.ncbi.nlm.nih.gov/pmc/articles/PMC2620621>.
- [36] G Poinar and AJ Boucot, *Parasitol* 133 (2006) <https://doi.org/10.1017/S0031182006000138>.
- [37] GO Poinar, *The Evolutionary History of Nematodes*, (2011) Brill, Leiden-Boston, ISBN: 978-90-04-17521-1.
- [38] GO Poinar, *Adv Parasitol* 90 (2015) <https://doi.org/10.1016/bs.apar.2015.03.002>.
- [39] GO Poinar and DC Currie, *Nematology* 22 (2020) <https://doi.org/10.1163/15685411-00003328>.
- [40] K De Baets et al., in *The Evolution and Fossil Record of Parasitism* 49 (2021) K De Baets and JW Huntley, eds, Springer, Cham. https://doi.org/10.1007/978-3-030-42484-8_7.
- [41] C Luo et al., *eLife* 12 (2023) <https://doi.org/10.7554/eLife.86283>.
- [42] T Aureliano et al., *Cretaceous Res* 118 (2021) <https://doi.org/10.1016/j.cretres.2020.104672>.
- [43] SH Holm et al., *Lab Chip* 11 (2011) <https://doi.org/10.1039/C0LC00560F>.
- [44] MR Samoiloff and J Pasternak, *Canadian J Zool* 47 (1969) <https://doi.org/10.1139/z69-109>.
- [45] M Armitage and J Solliday, *Microscopy Today* 28 (2020) <https://doi.org/10.1017/s1551929520001340>.
- [46] M Armitage, *Microscopy Today* 30 (2022) <https://doi.org/10.1017/s1551929522001262>.
- [47] MH Armitage, *Microscopy Today* 29 (2021) <https://doi.org/10.1017/S1551929521000468>.

MT



The PV-100 tabletop SEM from ModuleSci offers exceptional resolution in a compact package. Featuring a 5-axis stage and PICOSMART software, the PV series is the ideal solution when lab space is at a premium.

Modulesci.com • info@modulesci.com **MODULESCI**

Downloaded from <https://academic.oup.com/mt/article/32/1/26/7604511> by guest on 09 February 2024

Don't Let a Fingerprint Ruin Your Day—Use **Evactron**[®] Cleaning



Fingerprints are one of the major sources of contamination in vacuum systems. Evactron dual-action *turbo plasma cleaning*[™] expels these adventitious hydrocarbons with:

- ❖ Oxygen radicals plus UV active desorption
- ❖ Hollow cathode plasma radical source
- ❖ No kinetic sputter etch damage or debris
- ❖ A compact and efficient plasma source
- ❖ Cleaning in minutes for days of perfect imaging and analysis



**Need clean samples and chamber surfaces?
Let us show you the
“fastest way to pristine”[™]!**

WWW.EVACTRON.COM 1-650-369-0133